



Automatic detection and visualization system for coronary artery calcification using optical frequency domain imaging

Ryo Oikawa¹ • Akio Doi¹ • Masaru Ishida² • Basabi Chakraborty³

Received:

©

Abstract:

Percutaneous coronary intervention (PCI) is mainly used in the treatment of stenosis of the coronary arteries of the heart characteristic of coronary artery disease, and it is important that level of calcification is evaluated in advance of this procedure. A physician typically examines a cross-sectional angiogram and decides whether PCI is applicable. However, it takes a lot of time to interpret many sliced images. It is difficult to accurately assess the entire calcified area from the individual slices. To solve these problems, we propose an automatic detection and visualization system for coronary artery calcification by using images obtained from optical frequency domain imaging (OFDI). This system assists physicians by automatically detecting and intuitively visualizing calcified areas in a short period of time. The system is built using DeepLabv3+, a deep learning network for semantic segmentation. The deep neural network was trained using 2,149 coronary OFDI images labeled by physicians.

Keywords Deep Learning, Semantic Segmentation, Fully Convolutional Neural Network, OFDI image, Visualization.

1 Introduction

When a coronary artery is completely occluded due to acute coronary syndrome or chronic coronary artery disease, the mortality rate increases for every 15-minute delay in resumption of blood flow after one hour of blood flow interruption. It is considered critically important to achieve a blood flow recovery time of 2 hours or less from the onset of the disease, with a shorter occlusion time leading to a better prognosis. Percutaneous coronary intervention (PCI) is the most common revascularization procedure and is often used to treat blockages in coronary arteries. In PCI, a deflated balloon is

sent into the occluded artery, inflated to relieve the stenosis, and then a stent is implanted. However, in highly calcified lesions, stent underexpansion can be problematic, so it is important to assess the degree of calcification beforehand.

Intravascular ultrasonography (IVUS) and optical frequency domain imaging (OFDI) are the main techniques used to visualize the coronary artery lumen and vessel surface layers. In IVUS, by inserting a miniature ultrasound transducer mounted catheter into an artery, a cross-sectional image of the vessel wall can be obtained and assessed. While IVUS has excellent detection performance for coronary calcium deposits, it is impossible for IVUS to quantify the thickness of these deposits due to acoustic shadows [1][2].

In comparison with IVUS, OFDI is an intravascular diagnostic imaging system with a high resolution of 10–20 μm , and is based on near-infrared laser light and fiber-optic technology. It can be used to evaluate calcification with a spatial resolution ten times higher than IVUS and clear image quality. Along with IVUS, imaging modality has sufficient accuracy as a tool for detecting calcification [3], and in recent years it has been introduced at various facilities.

A physician first looks at the distribution of calcification, such as continuity, thickness, and intensity of calcified area, in order to determine if PCI can be applied, because heavy coronary calcification is a poor prognostic factor for PCI [4].

This work was presented in part at the 27th International Symposium on Artificial Life and Robotics, ONLINE, January 25–27, 2022.

✉ Akio Doi

doia@iwate-pu.ac.jp

¹ Faculty of Software and Information Sciences, Iwate Prefectural University, Iwate, Japan

² Department of Internal Medicine, Division of Cardiology, Iwate Medical University, Iwate, Japan

³ Dean of School of computing Sciences, Madanapalle Institute of Technology, AP, India, Distinguished Professor and Professor Emeritus, Iwate Prefectural University, Iwate, Japan

However, it takes time to read many high-resolution slice images, and the reliability of the diagnosis depends on the skill of the physician.

Therefore, we have developed a system that automatically detects calcified areas from OFDI images of coronary arteries. The system is built using DeepLabv3+ [5], a deep learning network for semantic segmentation. The deep neural network was trained using 2,149 coronary OFDI images labeled by physicians. The developed system can displays the distribution of calcification area in a more intuitive manner to aid in diagnosis.

In this system, arbitrary slice image display, volume rendering display, and easy selection of slice images, and so on, are possible. Diagnostic assistance is also provided by indicating calcification angles with arcs, and thicknesses with colors. The colored circle with the thickness of the calcified area is very effective to evaluate both the maximum value of the angle and thickness of the region where the calcification is continuous. In addition, the developed system can calculate the calcium volume index (CVI) defined by Fujino et al. [6], in order to objectively estimate whether there is stent underexpansion.

2 Related works

Recently, several machine learning approaches for detecting and classifying lesions from optical coherence tomography (OCT) images have been reported. He et al. developed a model for automatic plaque characterization from OCT images using convolutional neural networks [7]. Min et al. proposed detecting the thin-cap fibroatheroma using deep learning techniques from OCT images [8].

Additionally, Chu et al. developed a new AI framework that can automatically characterize plaque in images on a pixel by pixel basis, and integrated it into a commercial di

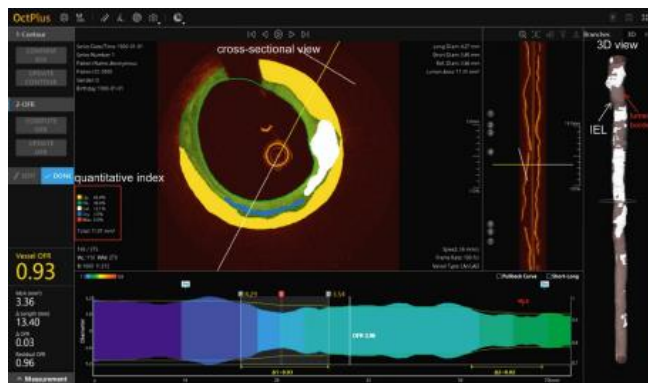


Fig. 1 The AI model proposed by Chu et al. was integrated into the OctPlus software. This is a screen shot of plaque quantitative assessments by the software

agnostic support system to achieve a highly accurate classification and display of lesions in vascular cross-sections (Fig. 1) [9].

Abbott Vascular Inc. (Santa Clara, CA) has also developed Ultreon 1.0, an AI-based software package for cardiovascular OCT diagnostic imaging systems. It displays calcified areas by drawing arcs around the cross-sectional view of the blood vessels (Fig. 2a) [10]. However, these interfaces provide an assessment of the continuity of calcified areas. Only the maximum thickness of calcified areas is displayed, no assessment of the thickness of other areas is available.

A calcium scoring system based on OCT was proposed by Fujino et al. in order to predict stent under expansion [6]. The calcification score is called CVI and is defined as 2 points for a maximum angle of $>180^\circ$, 1 point for a maximum thickness of >0.5 mm, and 1 point for a length of >5 mm. In the validation cohort of their study, it was reported that lesions with a CVI of 0 to 3 had excellent stent expansion, whereas lesions with a CVI of 4 had poor stent expansion. It was also reported that calcification with a maximum thickness of 0.5 mm or less can be dispersed and the blood vessel has spread normally during PCI [6]. The developed system calculated and displayed the CVI based on this definition.

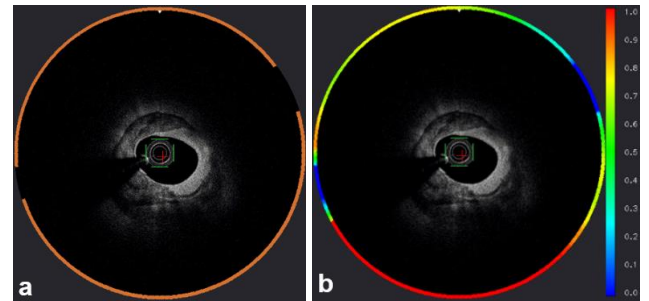


Fig. 2 a: The system displays the extracted calcified areas as orange rings. The figure was created with reference to Ultreon 1.0. b: Our newly proposed system. Thickness is indicated by color

3 System overview

The developed system consists of two functions: a function to detect calcified areas and a function to visualize the detected calcified areas. Fig. 3 shows an example of the visualization results for coronary artery calcification. The left image in Fig. 3 shows the detected calcified area overlaid on the original sliced image. The thickness of the calcified area is indicated by the color gradation of the outer ring.

Blue indicates less calcification and red indicates more calcification. The difference between our system and OctPlus or Ultreon 1.0 is that our system can directly display

the total thickness of the calcified area. The cross-sections can also be displayed interactively using the slide bar.

As shown in the right side of Fig. 3, this system supports display on mobile devices. The results of the visualization of coronary artery calcification areas can be sent to an Android device, and the interface can be operated in the same way as in the PC version.

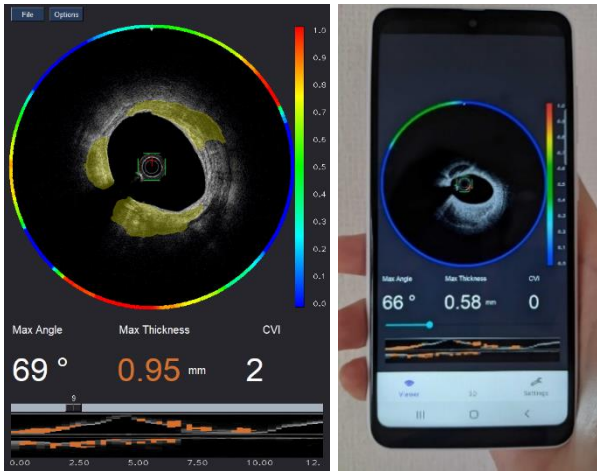


Fig. 3 User interface of the system for automatic detection and visualization of coronary artery calcification. In the PC version, load images from the button at the top left of the screen. In the Android version, the user can see the results transferred from the PC. Use the slider bar at the bottom of the screen to switch slices

Fig. 4 shows the entire flow of data and the various processing steps in the system. The image obtained with OFDI is sent to a data center via the Internet, and this data center automatically categorizes each sliced image using deep learning. More specifically, DeepLabv3+ is used to detect the calcified area from OFDI images. The images processed

at the data center are then sent to the user's computer for visualization.

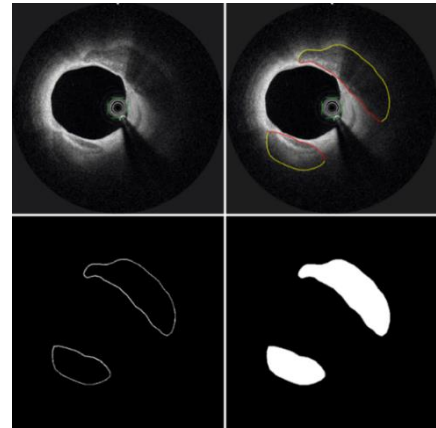


Fig. 5 Creating a labeled image. It is a binary label for calcification and background

4 Automatic Detection

4.1 Detection of the calcified regions

To detect the calcified regions, we adopted deep learning network for semantic segmentation [11]. The automatic detection of calcified areas is performed in the following steps: data preparation, model training, and segmentation of calcified areas using the trained model.

The dataset used for training consists of 2,149 coronary OFDI images labeled by physicians. For labeling, the physician traces the inner boundary in red and the outer boundary in yellow, and then two experts cross-check the results. Each line segment constitutes a closed boundary, and the calcified area is automatically filled in from this boundary (Fig. 5). The labeled images used in training increase the amount of

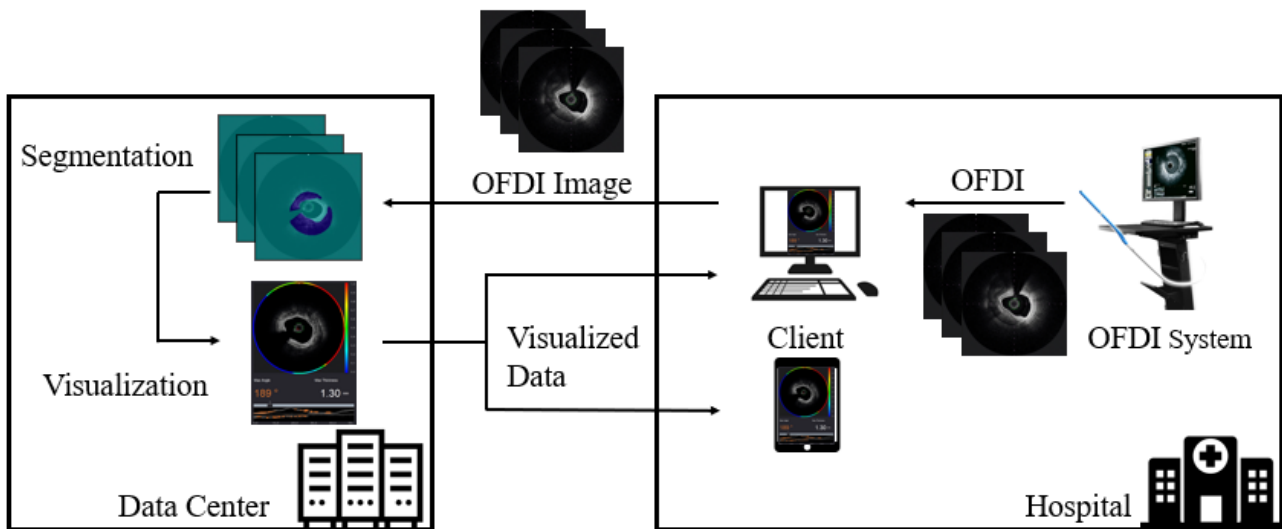


Fig. 4 Dataflow and processing steps for OFDI image classification.

data to improve accuracy. Specifically, we also applied flips and rotations (8 different rotations of 45 degree increments) to increase the amount of data by a factor of 16 (Fig. 6).

DeepLabv3+, a network for segmentation, was used for detecting the calcified regions. The network is shown in Fig. 7. This network is a type of DilatedFCN and achieved state-of-the-art semantic segmentation performance in 2018 [5].

DilatedFCN achieves a high receptive field by using dilated convolution, which is a method of convolving while extending the filter's range of application. Therefore, it can capture global features with a small number of parameters. By layering these dilated convolution layers in a pyramid shape (ASPP: Atrous Spatial Pyramid Pooling), DeepLabv3+ enables highly accurate segmentation and detection of features at arbitrary resolutions. ResNet-50 [12] was used as a backbone network of DeepLabv3+, in order to detect the calcified area efficiently. ResNet-50 is a convolutional neural network that is 50 layers deep. We used a pre-trained version of the network trained on more than a million images from the ImageNet database [13].

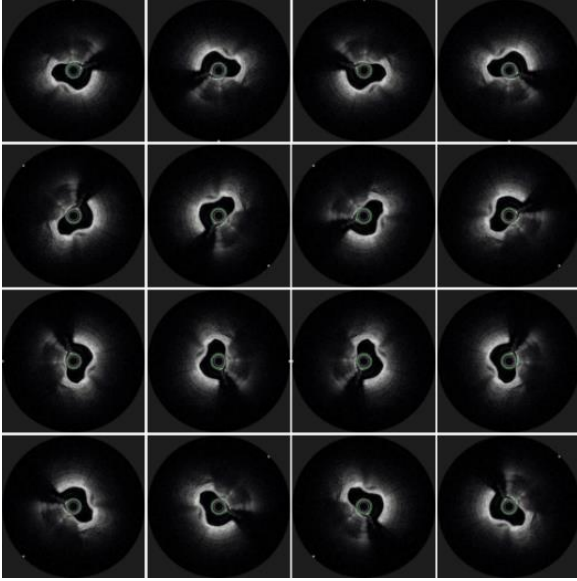


Fig. 6 Data augmentation via flips and rotations

4.2 Thickness calculation

In order to calculate thickness of calcified areas, it is necessary to remove artifacts such as catheters, guidewires, and crosshairs drawn by the OFDI diagnostic imaging equipment, which name is LUNAWAVE, Terumo Corporation [14]. Of these, the catheter is generally visible in the center of the OFDI images because during OFDI, the catheter is shifted along the guidewire inserted into the blood vessel (Fig. 8a). We applied binarization to the OFDI images using the Otsu thresholding method (Fig. 8b) and then removed the pixels

in the central area where the catheter was likely to be (Fig. 8c).

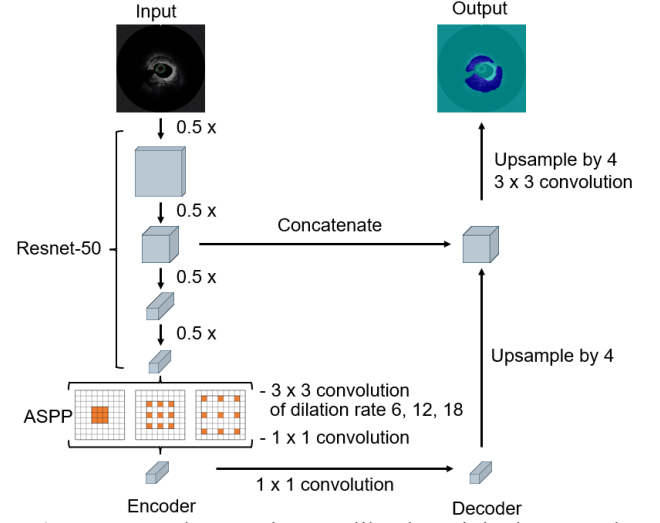


Fig. 7 Network Overview. Unlike the original proposal for DeepLabv3+, this network does not include a global average pooling layer in the ASPP

In Otsu's discriminant analysis method, when a histogram is classified into two classes by the threshold value t , the numbers of pixels in each group are $\omega_1(t)$ and $\omega_2(t)$, and their averages are $m_1(t)$ and $m_2(t)$, respectively. Then, the threshold value t that maximizes the reference Eq. (1) is calculated.

$$\omega_1(t)\omega_2(t)(m_1(t) - m_2(t))^2 \quad (1)$$

It has been reported that this threshold value t has a bias when there is a large difference in the number of distributions belonging to each class, but since there is no extreme difference between the black and white areas in the OFDI images, this method is used [15][16].

A median filter is then used to remove the guidewire (crescent-shaped signal on the side of the catheter) and the crosshairs (Fig. 8d).

Additionally, since the guidewire reflects light, a shadow is created in the region behind it. It is desirable to detect this shadow and exclude it from the thickness calculations. The shadowed region is detected by scanning the pixels radially from the center of the image to the periphery (Fig. 8e).

It is necessary to calculate the thickness of the calcification by using the lumen center of the vessel instead of the image center. Since the luminal center is equal to the center of gravity of the luminal region, we construct a closed boundary for the vessel wall by connecting the non-zero pixels detected in the scanning described above, and then find the center of gravity of the area obtained by filling in the

boundary (Fig. 8f). Using these data, we visualize the detected calcified area.

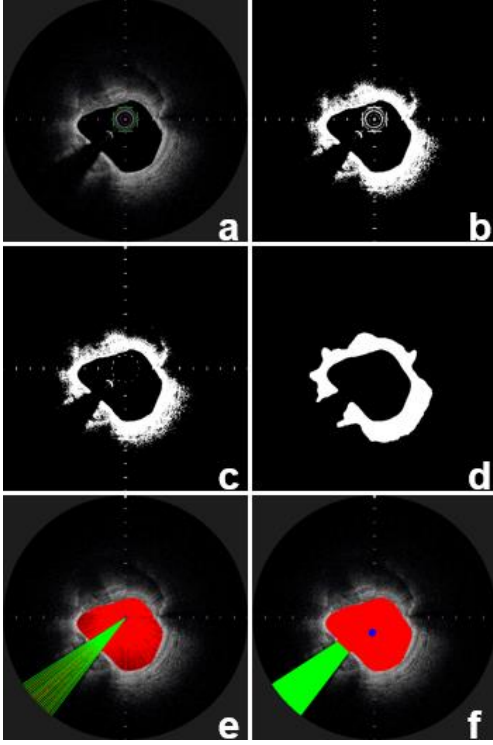


Fig. 8 Detection of guidewire shadow and lumen center. f) The red area is the vessel lumen, the green area is the shadow of the guidewire, and the blue point is the center of the vessel

4.3 Visualization of calcified area

The thickness of the calcification is calculated radially, at a fixed angle, using the center of the vessel lumen as the origin. From this calculation, the maximum value of the angle and thickness of the region where the calcification is continuous is obtained (Fig. 9).

Based on the results from the processing step shown in Fig. 8f, the vessel lumen area and the area shaded by the guidewire are excluded from the calculation. The thickness, $d(\theta)$, is the thickness of the calcified area from the center of the vessel lumen at an angle θ and is defined by Eq. (2):

$$d(\theta) = \alpha \sum_{r=0}^L S(P) \quad (2)$$

$$S(P) = \begin{cases} 1 & \text{if } P(rcos\theta, rsin\theta) \text{ is calcified} \\ 0 & \text{if } P(rcos\theta, rsin\theta) \text{ is not calcified} \end{cases} \quad (3)$$

Here, P is the pixel position, r is the distance from the origin, θ is the angle shown in Fig. 9, and $S(P)$ is a function that returns 1 for calcification and 0 for non-calcification. Additionally, α is an adjustment factor to convert between image space and distance, and is calculated from the pixel length of the calcified area and the image size.

As shown in Fig. 9, the lumen center, which is the center of the vessel, and the catheter center, which is the center of the image, are different and must be calculated in the manner described in this section.

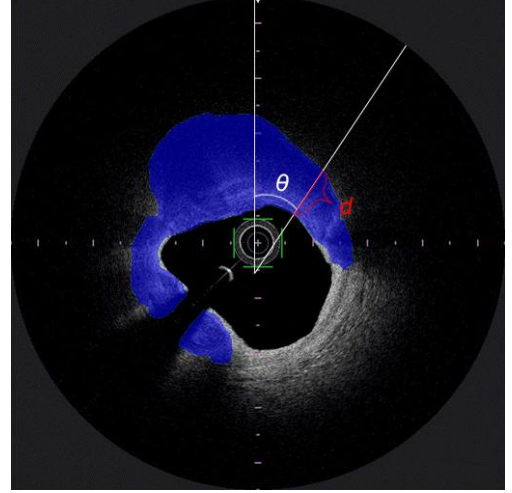


Fig. 9 Calculating the thickness of calcification as a function of the angle. The blue area is the calcified area and the red area indicated by the symbol d is the thickness calculated from the lumen center

The method we developed also displays a circle colored according to the thickness of the calcified area. The color space is calculated using the HSV color system (Fig. 10), and finally is converted to the RGB color system. H represents the hue, which is calculated using Eq. (4).

$$H = H_{max} * (1 - (d(\theta)/d_{max})), \quad 0 \leq H \quad (4)$$

The constant H_{max} , which represents the maximum value of H , is set to 240 (blue). d_{max} is a constant that represents the maximum range of thicknesses to be colored. The d_{max} was set at 1.0 mm because it is important to know if there is calcification with a thickness greater than 0.5 mm. Therefore, H is 0 (red) in regions where $d(\theta)$ is thicker than 1.0 mm.

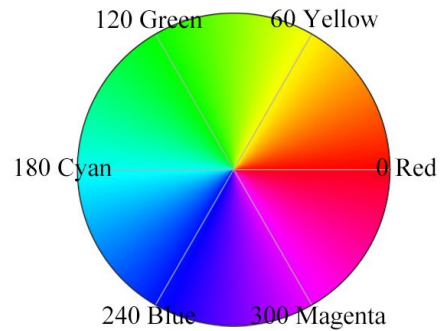


Fig. 10 The hue value wheel used for calculations
The overall algorithm for calculating the color is described

in Algorithm 1. The RGB color for a thickness $d(\theta)$ is defined by C, and `hsv_to_rgb` is a function to convert the color space from HSV to RGB.

Algorithm 1 Algorithm for Color

- 1: $H = H_{max} * (1 - (d(\theta)/d_{max}))$
 - 2: **if** ($H < 0$) **then**
 - 3: $H = 0$
 - 4: **end if**
 - 5: $C = \text{hsv_to_rgb}(h, 255, 255)$
-

The final visualization results from the obtained data are shown in Fig. 11. The threshold value, d_{max} , is set to 1.0. Areas with no calcification are marked in blue, and areas with significant calcification are marked in red. On the user interface, “Max Angle” is the maximum angle at which calcification is continuous, and “Max Thickness” is the maximum value of the thickness.

4.4 Volume visualization of calcified areas

Volume rendering is a useful tool for displaying the entire calcified area. After detecting the calcified regions from the stacked OFDI images, calcified regions are displayed in real time. Various visualizations are possible by adjusting the transfer function of volume rendering (Fig. 12).

Volumes can also be visualized on wearable devices such as smart glasses, as shown in Fig. 13. By displaying information at the physician's eye, it is expected that the physician can proceed with the surgery without taking their eyes off the operating field.

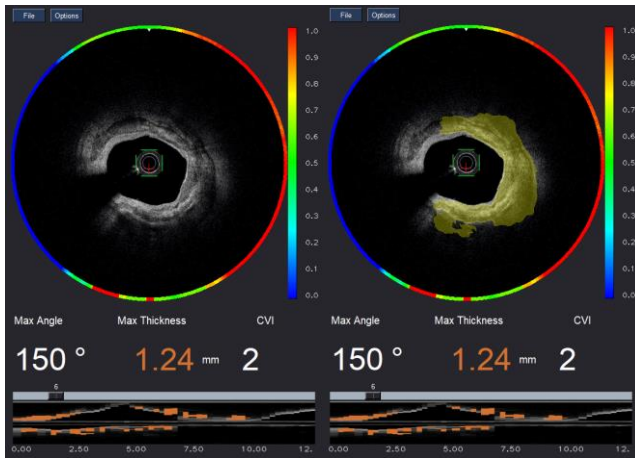


Fig. 11 Example visualization of a calcified area. The colored circle indicates the thickness of the calcified area in color. The left image shows the segmentation results without display and the right image shows the segmentation results

with display. The image at the bottom of the screen is a longitudinal section of a blood vessel, and the orange area is the calcified region

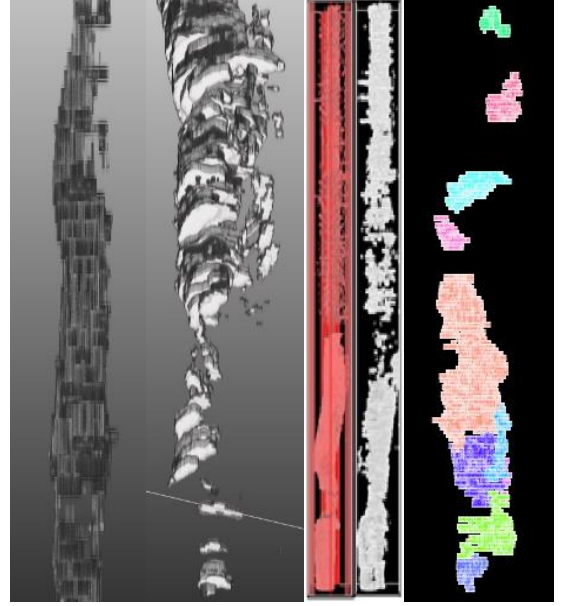


Fig. 12 Example volume rendering of calcified areas. The image on the left is volume rendered with Joint Vision and the image on the center is volume rendered with Volume Extractor. The image on the right shows a 3D Viewer display after the area was divided using ImageJ's MorphoLibJ plugin



Fig. 13 Example volume visualization using smart glasses. The white areas are calcified areas

5 Evaluation

5.1 Quantitative evaluation of segmentation results

The Jaccard similarity coefficient (JSC) and the Dice similarity coefficient (DSC) are commonly used indices in the field of computer vision to quantitatively evaluate segmentation results [17]. Therefore, JSC, DSC and accuracy are used for quantitative evaluation in this paper.

JSC and DSC are defined as in Eq. (5) and (6).

$$\text{Jaccard similarity coefficient} = \frac{TP}{TP + FP + FN} \quad (5)$$

$$\text{Dice similarity coefficient} = \frac{2 \cdot TP}{2 \cdot TP + FP + FN} \quad (6)$$

5.2 Computing results, environment and time

The prediction results of the model used in the experiment are shown in Fig. 14. The predictions of the model used in the experiment are shown in Figure 14. From left to right: original image, ground-truth, DeepLabv3+ predicted image, U-Net predicted image, and FCN predicted image. The dark blue part of the image shows the calcified area, and the other part shows the non-calcified area. The validation environment is summarized in Table 1. The development environment for the PC version of the developed system is summarized in Table 2, and the development environment for the Android device version is summarized in Table 3.

As shown in Fig. 14a, b, c, d, e, f, the model with DeepLabv3+ was able to accurately detect calcified area. There were a few cases with many false-negative pixels, as in Fig. 14g, and a few cases with many false-positive pixels, as in Fig. 14h. There were four cases in which the AI recognized more than 3 mm² more area as calcium than the correct answer, and two cases in which it recognized more than 3 mm² less. Possible causes of such recognition errors include blood clots and the effects of non-calcium plaques. In some cases, a portion of the vessel lumen was recognized as calcium, as in Fig. 14i. In this case, these portions were excluded from the calculation as shown in Section 4.3, so it did not affect the final visualization results as shown in Fig. 3 and Fig. 11.

JSC, DSC, and accuracy in DeepLabv3+ are shown in Table 4. The segmentation accuracy of the calcified area was 83%. The reason for the good recognition accuracy of the background is due to the large number of pixels in the background. JSC were lower than DSC because they are indices that strictly evaluate the position of the target, omission of contours, and slight overhang. In comparison with the conventional methods, this model was the best in both JSC and DSC. A comparison of JSC and DSC are shown in Tables 5 and 6.

The time required for training, the average prediction time per image, and the average calcification visualization time per image are shown in Table 7. The calcification visualization time is measured from just before the Segmented OFDI image is loaded until the resulting image is saved on the server. For a single image, prediction can be done in about 1.15 seconds and visualization in about 1.61 seconds.

Table 1 Validation environment

CPU	Intel® Core™ i9-9940X
RAM	128GB (16GB×8)
GPU	NVIDIA QUADRO RTX 8000 ×4
OS	Ubuntu 18.04 LTS
Patients	44
Image size	512×512 pixels
Training data	31,184
Test data	200
Epochs	500
Minibatch size	32
Initial learning rate	0.0001
Optimizer	Adam

Table 2 PC version development environment

Language	Python 3.8.10
Testing device	Windows PC
OS Version	21H1 (Build 19043.1826)

Table 3 Android version development environment

Language	Kotlin
Testing device	Samsung Galaxy A22 5G SC-56B
API Level	31
IDE	Android Studio Bumblebee 2021.1.1 Patch 3

Table 4 JSC, DSC, and accuracy

	Calcium	Background
JSC	0.59	0.97
DSC	0.72	0.98
Accuracy	0.83	0.98

Table 5 Comparison of JSC by model

	Calcium	Background
DeepLabv3+	0.59	0.97
U-Net	0.40	0.92
FCN	0.47	0.94

Table 6 Comparison of DSC by model

	Calcium	Background
DeepLabv3+	0.72	0.98
U-Net	0.55	0.93
FCN	0.62	0.97

Table 7 Computational time (seconds)

Training time	258,464
Prediction time	1.15 per image
Visualization of calcified areas	1.61 per image

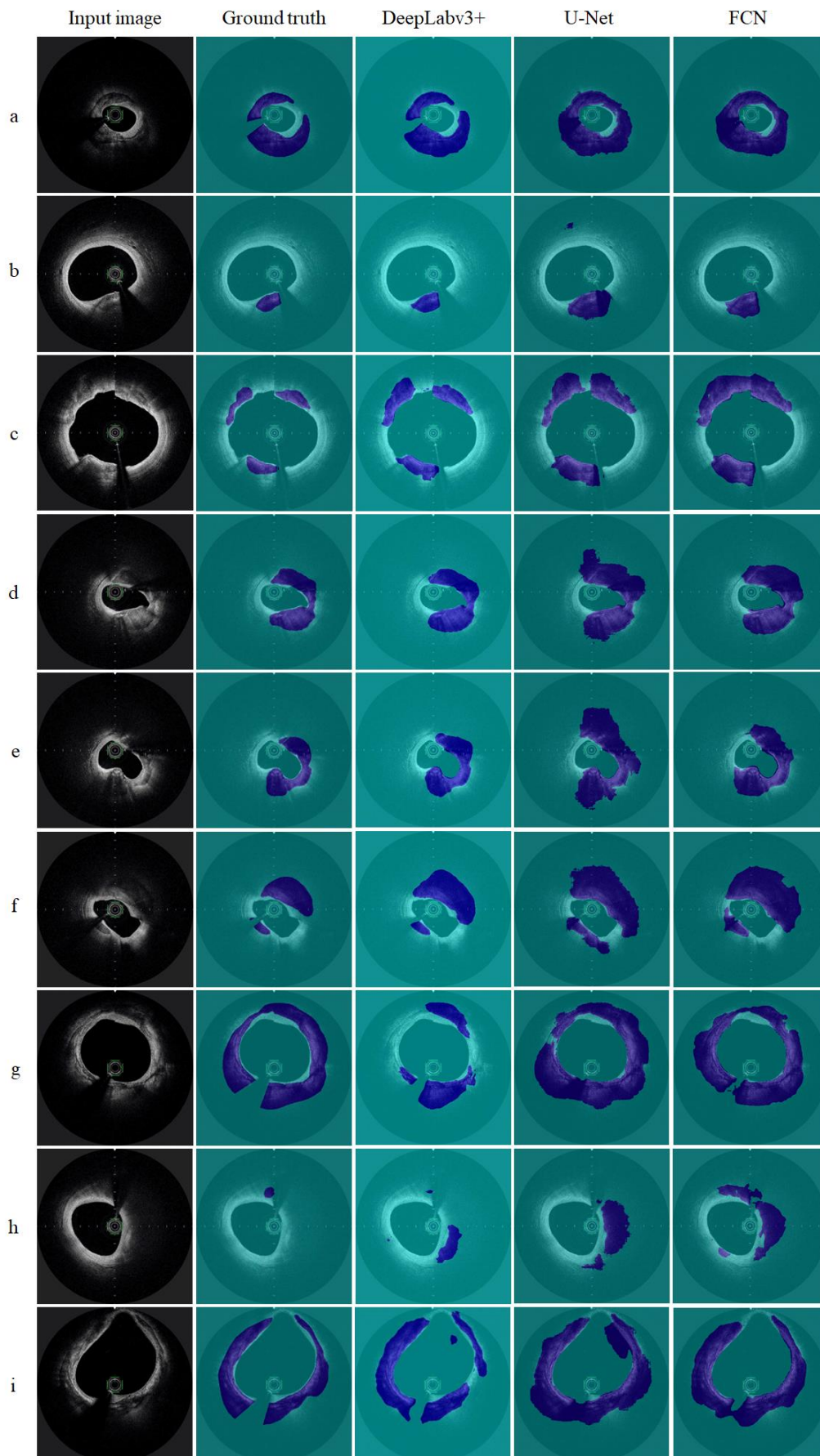


Fig. 14 Prediction result

This research was partly supported by a Grant-in-Aid for Scientific Research (C) from the Japan Society for the Promotion of Science (grant number JP20K08142), as well as

by the "FY2022 Research and Development Subsidy Program" of the Japan Keirin Autorace (JKA) Foundation and the "FY2020 Iwate Strategic Research and Development Promotion Program" of Iwate Prefecture. We would like to express our gratitude to these organizations.

References

- [1] A. Maehara, M. Matsumura, Z. A. Ali, G. S. Mintz, and G. W. Stone, "IVUS-Guided Versus OCT-Guided Coronary Stent Implantation: A Critical Appraisal", *JACC Cardiovasc Imaging*, Vol. 10, No. 12, pp. 1487-1503, 2017.
- [2] X. Wang, M. Matsumura, G. S. Mintz, T. Lee, W. Zhang, Y. Cao, A. Fujino, Y. Lin, E. Usui, Y. Kanaji, T. Murai, T. Yonetsu, T. Kakuta, and A. Maehara, "In Vivo Calcium Detection by Comparing Optical Coherence Tomography, Intravascular Ultrasound, and Angiography", *JACC Cardiovasc Imaging*, Vol. 10, No. 8, pp. 869-879, 2017.
- [3] A. Fujino, G. S. Mintz, T. Lee, M. Hoshino, E. Usui, Y. Kanaji, T. Murai, T. Yonetsu, M. Matsumura, Z. A. Ali, A. Jeremias, J. W. Moses, R. A. Shlofmitz, T. Kakuta, and A. Maehara, "Predictors of calcium fracture derived from balloon angioplasty and its effect on stent expansion assessed by optical coherence tomography", *JACC Cardiovasc Interv*, Vol. 11, No. 10, pp. 1015-1017, 2018.
- [4] P. Guedeney, B. E. Claesse, R. Mehran, G. S. Mintz, M. Liu, S. Sorrentino, G. Giustino, S. Farhan, M. B. Leon, P. W. Serruys, P. C. Smits, C. von Birgelen, Z. A. Ali, P. G  n  reux, B. Redfors, M. V. Madhavan, O. Ben-Yehuda, and G. W. Stone, "Coronary Calcification and Long-Term Outcomes According to Drug-Eluting Stent Generation", *JACC Cardiovasc Interv*, Vol. 13, No. 12, pp. 1417-1428, 2020.
- [5] L.-C. Chen, Y. Zhu, G. Papandreou, F. Schroff, and H. Adam, "Encoder-Decoder with Atrous Separable Convolution for Semantic Image Segmentation", In *ECCV*, 2018.
- [6] A. Fujino, G. S. Mintz, M. Matsumura, T. Lee, S. Y. Kim, M. Hoshino, E. Usui, T. Yonetsu, E. S. Haag, R. A. Shlofmitz, T. Kakuta, and A. Maehara, "A new optical coherence tomography-based calcium scoring system to predict stent underexpansion", *EuroIntervention*, Vol. 13, No. 18, pp. 2182-2189, 2018.
- [7] S. He, J. Zheng, A. Maehara, G. S. Mintz, D. Tang, M. Anastasio, and H. Li, "Convolutional neural network based automatic plaque characterization from intracoronary optical coherence tomography images", *Medical Imaging 2018: Image Processing* 107, 2018.
- [8] H.-S. Min, J. H. Yoo, S.-J. Kang, J.-G. Lee, H. Cho, P. H. Lee, J.-M. Ahn, D.-W. Park, S.-W. Lee, Y.-H. Kim, C. W. Lee, Seong-Wook Park, and Seung-Jung Park, "Detection of optical coherence tomography-defined thin-cap fibroatheroma in the coronary artery using deep learning", *EuroIntervention*, Vol. 16, No. 5, pp. 404-412, 2020.
- [9] M. Chu, H. Jia, J. L. G.-Chico, A. Maehara, Z. A. Ali, X. Zeng, L. He, C. Zhao, M. Matsumura, P. Wu, M. Zeng, T. Kubo, B. Xu, L. Chen, B. Yu, G. S. Mintz, W. Wijns, MD, N. R. Holm, and S. Tu, "Artificial intelligence and optical coherence tomography for the automatic characterisation of human atherosclerotic plaques", *EuroIntervention*, Vol. 17, No. 1, pp. 41-50, 2021.
- [10] ULTREONTM 1.0 SOFTWARE Website, <https://www.cardiovascular.abbott/int/en/hcp/products/percutaneous-coronary-intervention/intravascular-imaging/ultreon-software/about.html>
- [11] R. Oikawa, T. Kato, A. Doi, B. Chakraborty, and M. Ishida, "Extraction of Calcified Regions from OCT Images Using Deep Learning", *IEICE-MI2021-12*, pp.15-19, 2021.
- [12] K. He, X. Zhang, S. Ren, and J. Sun, "Deep residual learning for image recognition", In *CVPR*, pp. 770-778, 2016.
- [13] O. Russakovsky, J. Deng, H. Su, J. Krause, S. Satheesh, S. Ma, Z. Huang, A. Karpathy, A. Khosla, M. Bernstein, et al., "Imagenet large scale visual recognition challenge", *IJCV*, 115(3):211-252, 2015.
- [14] LunawaveTM Coronary Optical Coherence Tomography Imaging System Website, <https://www.terumo-europe.com/en-emea/products/lunawave%E2%84%A2-coronary-optical-coherence-tomography-imaging-system>
- [15] N. Otsu, "An automatic thresholding based on discrimination and least squares criteria", *Transactions of the Institute of Electronics and Communication Engineers of Japan (D)*, Vol. J63-D, No. 4, pp. 349-356, 1980 (in Japanese).
- [16] J. Kittler and J. Illingworth, "Minimum Error Thresholding", *Pattern Recognition*, Vol. 19, No. 1, pp. 41-47, 1986.
- [17] Shervin Minaee, Yuri Boykov, Fatih Porikli, Antonio Plaza, Nasser Kehtarnavaz, and Demetri Terzopoulos, "Image Segmentation Using Deep Learning: A Survey", *arXiv:2001.05566*, 2020.
- [18] J. M. Hill, D. J. Kereiakes, R. A. Shlofmitz, A. J. Klein, R. F. Riley, M. J. Price, H. C. Herrmann, W. Bachinsky, R. Waksman, G. W. Stone, and on behalf of the Disrupt CAD III Investigators, "Intravascular Lithotripsy for Treatment of Severely Calcified Coronary Artery Disease", *JACC*, Vol. 76, No. 22, pp. 2635-2646, 2020.
- [19] G. L. De Maria, R. Scarsini, and A. P. Banning, "Management of Calcific Coronary Artery Lesions: Is it Time to Change Our Interventional Therapeutic Approach?", *JACC: Interventions*, Vol. 12, No. 15, pp. 1465-1478, 2019.
- [20] I. Goodfellow, J. Pouget-Abadie, M. Mirza, B. Xu, D. Warde-Farley, S. Ozair, A. Courville, Y. Bengio, "Generative Adversarial Nets", *NIPS*, 2014.
- [21] S. Iizuka, E. Simo-serra, H. Ishikawa, "Globally and Locally Consistent Image Completion", *ACM Transactions on Graphics*, Vol. 36, No. 4, pp. 1-14, 2017.